



## Experimental realization of a 12,000-finesse laser cavity based on a low-noise microstructured mirror

Johannes Dickmann<sup>1</sup>  <sup>✉</sup>, Steffen Sauer<sup>1</sup>, Jan Meyer<sup>1</sup>, Mika Gaedtke<sup>1,2</sup>, Thomas Siefke<sup>3</sup>, Uwe Brückner<sup>4</sup>, Jonathan Plentz<sup>4</sup>  & Stefanie Kroker<sup>1,5</sup>

The most precise measurement tools of humankind are equipped with ultra-stable lasers. State-of-the-art laser stabilization techniques are based on external cavities, that are limited by noise originated in the coatings of the cavity mirrors. Microstructured mirror coatings (so-called meta-mirrors) are a promising technology to overcome the limitations of coating noise and therewith pave the way towards next-generation ultra-stable lasers. We present experimental realization of a 12,000-finesse optical cavity based on one low-noise meta-mirror. The use of the mirrors studied here in cryogenic silicon cavities represents an order of magnitude reduction in the current limiting mirror noise, such that the stability limit due to fundamental noise can be reduced to  $5 \times 10^{-18}$ .

<sup>1</sup>Technical University of Braunschweig, Institute for Semiconductor Technology, Hans-Sommer-Str. 66, 38106 Braunschweig, Germany. <sup>2</sup>Leibniz University Hannover, Welfengarten 1, 30167 Hannover, Germany. <sup>3</sup>Friedrich Schiller University Jena, Institute of Applied Physics, Albert-Einstein-Strasse 15, 07745 Jena, Germany. <sup>4</sup>Leibniz Institute of Photonic Technology (Leibniz-IPHT), Department Functional Interfaces, Albert-Einstein-Strasse 9, 07745 Jena, Germany. <sup>5</sup>Physikalisch-Technische Bundesanstalt, Bundesallee 100, 38116 Braunschweig, Germany. ✉email: [j.dickmann@tu-braunschweig.de](mailto:j.dickmann@tu-braunschweig.de)

On September 14, 2015, Earth was passed by a gravitational wave that could be detected by the two Laser Interferometer Gravitational-Wave Observatories (LIGO) with a signal of  $1.0 \times 10^{-21}$  (see refs. 1–5). The hearts of the LIGO detectors are ultra-stable lasers, implemented with the help of high-finesse laser cavities<sup>5,6</sup>.

In addition to gravitational wave detectors, the use of optical cavities makes it possible to address other questions in physics and technology: For example, the search for dark matter<sup>7–9</sup>, would be pushed by the implementation of a global network of optical atomic clocks<sup>10</sup>, also enabled by high-finesse cavities<sup>11–13</sup>.

Besides these applications in modern physics, there are several applications of laser cavities in modern technology like novel radar applications<sup>14,15</sup> and deep-space navigation<sup>16,17</sup>.

The best cavities today are made of monocrystalline silicon paired with highly reflective mirrors in Bragg technology<sup>6,18</sup>, see Fig. 1. These systems achieve  $4 \times 10^{-17}$  frequency stability over a broad frequency spectrum at a temperature of 124 K<sup>18</sup> by clever suppression of all relevant noise sources such as spacer noise<sup>19</sup>, vibration<sup>20</sup>, temperature fluctuations and quantum noise<sup>21</sup>. However, further improving the stability of lasers has become more challenging for several years, since current systems are fundamentally limited by Brownian noise<sup>6,18</sup>. This limitation can only be overcome by another mirror technology. One possibility is to use other materials, especially crystalline mirror layers, instead of the currently used amorphous materials<sup>22</sup>. These crystalline Bragg mirrors (see Fig. 2a) show a tenfold reduction of coating noise due to a lower mechanical loss compared to amorphous Bragg mirrors at room temperature<sup>22</sup>. However, a further reduction of thermal noise is not expected, because the limiting coating noise is proportional to the thickness of the

Bragg layer stack<sup>23</sup>. The total thickness of these crystalline mirror layers is generally higher than that of their amorphous counterparts due to smaller refractive index contrasts of the materials that can be used. In addition, the advantages of crystalline Bragg mirrors disappear at cryogenic temperatures<sup>24</sup>, so another technology has to be explored.

Here, we report on the experimental realization of a high-finesse optical cavity based on a low-noise meta-mirror. In this case, not only the material has been changed, but the reflection mechanism itself. Meta-mirrors consist of one single layer of laterally structured material<sup>25,26</sup>, see Fig. 2b. The noise of these mirrors has been studied intensively<sup>27,28</sup>. We show that the use of silicon meta-mirrors reduces the coating noise by more than two orders of magnitude and the use of diamond almost by four orders of magnitude<sup>28</sup>. Until now, meta-mirrors could not be used for cavities because the achieved reflectivity of 99.8% (finesse 1500)<sup>29</sup> is not sufficient to stabilize a laser up to the ultimate thermal noise limit (details in the Results section Stability Calculation). To overcome this limitation, the concept of a two-mirror system, the so-called meta-etalon was developed<sup>30</sup>, see Fig. 2c. The meta-etalon combines the advantages of both mirror technologies: The high reflectivity of Bragg mirrors and the low thermal noise of meta-mirrors<sup>30</sup>. In this work, we present the first experimental realization of a meta-etalon and its application in a high-finesse optical cavity.

## Results

**Design of the low-noise meta-mirror.** The most stable laser cavities are typically operated at a wavelength of  $\sim 1550$  nm<sup>18,19</sup>. Thus, we also conducted experiments at this wavelength. The meta-mirror consists of a structured layer of amorphous silicon<sup>31</sup> on a fused silica substrate, see Fig. 2c. Rigorous coupled-wave analysis<sup>32,33</sup> was utilized to optimize the geometrical parameters of the meta-mirror, yielding a period  $\Lambda = 942$  nm, width  $W = 281$  nm and thickness  $H = 176$  nm. The reflective coatings of the meta-etalon are applied to a fused silica substrate with a thickness of 1.066 mm. The front surface of the substrate is covered with a silicon coating with a thickness of  $176 \pm 5$  nm, structured with the parameters above. The rear surface was contacted with a Bragg reflector consisting of ten quarter-wavelength pairs of alternating silicon dioxide/tantalum pentoxide layers, leading to a reflectivity of 99.5%. The two-mirror system forms an optical resonator with a free spectral range of 760 pm and a Finesse of  $\sim 300$ . To guarantee a high reflectivity of the whole etalon, this system has to be operated in antiresonance<sup>34,35</sup>. Experimentally, this is achieved by choosing the cavity length significantly larger than the etalon length. In this work, we investigated a 6-cm-long cavity, corresponding to a free spectral range of 20 pm, which is more than one order of magnitude smaller than the free spectral range of the etalon, whereby many resonances of the cavity are located in one antiresonance of the etalon. Thus, the antiresonance in the etalon can be maintained experimentally by simply stabilizing the temperature of the etalon substrate.

The high-finesse cavity comprising an etalon studied here is a very complex system. Thus, it is sensible to characterize the etalon separately before considering the entire system.

**Pre-characterization of the meta-etalon.** The transmissivity of the meta-mirror is strongly polarization-dependent since its structure is strongly anisotropic. Figure 3 shows scanning electron microscope images of the fabricated silicon meta-mirror. Details on the fabrication of the meta-mirror can be found in the methods section. To pre-characterize the fabricated etalon, we performed a wavelength- and polarization-dependent transmission measurement. This measurement

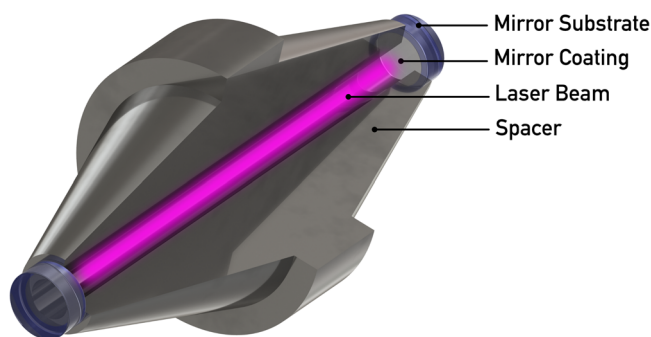


**Fig. 1 Artistic representation of a high-finesse optical cavity.** Shown is a laser stabilization cavity consisting of spacer, mirrors and coatings. Based loosely on ref. 18.

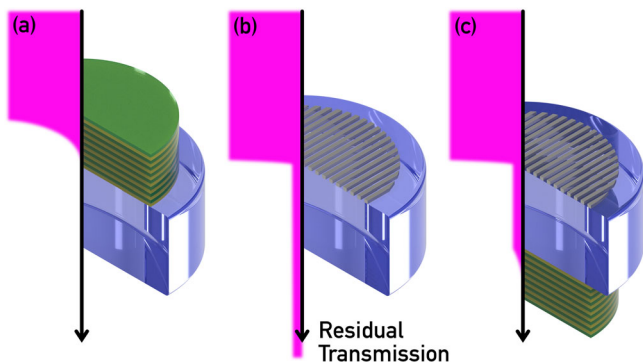


**Fig. 2 Scheme of the different mirror technologies.** **a** Conventional Bragg Mirror, **b** Meta-Mirror, **c** Meta-Etalon. The pink color indicates the intensity distribution in front of, inside and behind the mirror.

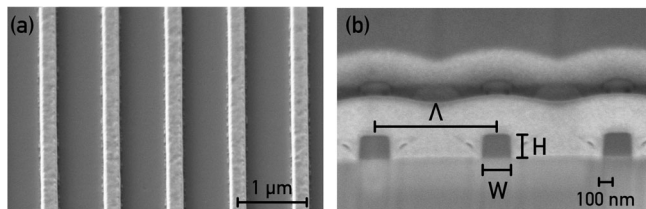


**Fig. 3** Scanning electron microscope images of the fabricated silicon meta-mirror. **a** Top view, **b** side view.  $\Lambda$  is the period of the structure,  $W$  is the width, and  $H$  is the thickness.

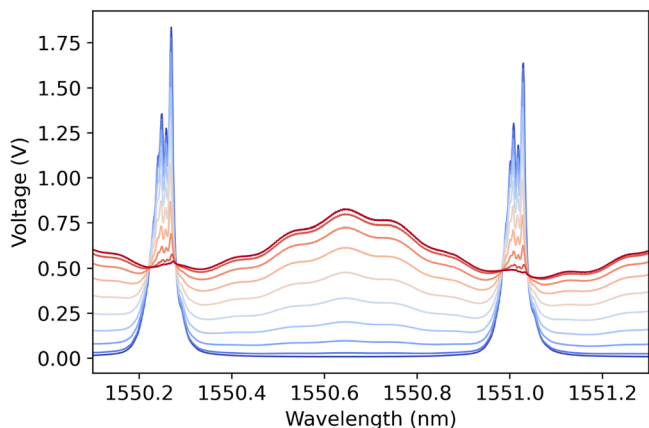


**Fig. 4** Measured transmittance of the meta-etalon versus wavelength of the incident light. The different colors indicate nine different angles of the linear polarized light between transverse electric (electric field parallel to structure, blue color, bottom line) and transverse magnetic polarized light (magnetic field parallel to structure, red color, top line).

was performed with a Keysight 81608A tunable laser source at an output power of 10 mW. The polarization of the incident light was rotated with a waveplate. Figure 4 shows the results in terms of photodiode voltage in transmittance as a measure of transmitted intensity. This plot shows nine different polarization angles between transverse electric (electric field parallel to structure, blue color) and transverse magnetic polarized light (electric field parallel to structure, red color). For transverse-electric polarized light, the transmittance shows the typical behavior of Fabry–Perot resonators: There are several resonant modes indicated by high transmittance and a broad spectral range between the resonances, where the transmittance is close to zero. This anti-resonant spectral range is the region of high etalon reflectivity. The transmitted light between the resonances increases for polarization angles different from transverse-electric polarization. This phenomenon arises due to the decreasing reflectivity of the meta-mirror for these polarizations. Using this polarization dependence, the etalon reflectivity can be tuned continuously.

**Finesse measurement.** The finesse of our optical cavity based on the meta-etalon was measured using cavity ring-down<sup>36–38</sup>. The measurement setup is shown in Fig. 5. The wavelength tunable laser source is used, such that the light power at the cavity input is 10 mW. The laser light is guided through a fiber-coupled acousto-optic modulator, which is used as an optical switch. After the light has been collimated to free space, it is directed into the 6-cm-long cavity consisting of an amorphous Bragg reference mirror with transmission less than ten parts per million and the meta-mirror under investigation. The rotating waveplate is used to adjust the polarization of the incident light. The measurement of cavity finesse works as follows: The laser frequency is detuned slowly.

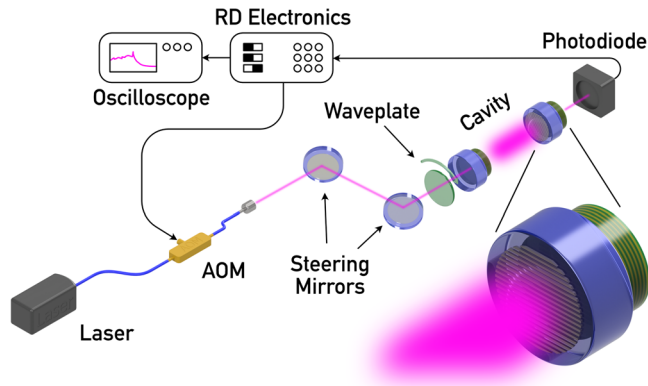


**Fig. 5** Cavity ring-down setup for the measurement of cavity finesse. Once a mode builds up in the cavity, the photodiode voltage exceeds a certain threshold. The ring-down (RD) electronics interrupt the laser light by the acousto-optic modulator (AOM). The temporally decreasing light intensity is measured with an oscilloscope.

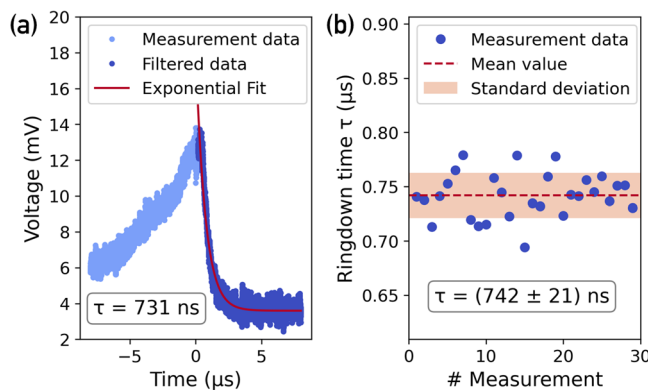


**Fig. 6** Measurement results of the cavity ring-down experiment. **a** One measured ring-down, **b** All 29 ring-down times, mean value and standard deviation.

Once, the frequency matches a resonance in the cavity, the transmitted intensity rises. The self-developed ring-down (RD) electronics switches the AOM as soon as the photodiode voltage exceeds a certain threshold. The light stored in the cavity leaves the cavity through the mirrors. This temporally decreasing light intensity is measured with an oscilloscope. The ring-down time  $\tau$ , i.e., the time when the light intensity has dropped to  $1/e$  of the initial intensity, is a measure for the cavity finesse<sup>34,39</sup>:

$$\mathcal{F} = \frac{\pi c}{L} \tau, \tag{1}$$

where  $c$  is the speed of light and  $L$  the cavity length, respectively. The temperature of the etalon substrate was stabilized and the laser wavelength was tuned within the antiresonance of the etalon (compare Fig. 4). The ring-down was measured 29 times for the fundamental cavity mode. Figure 6a shows one of the temporally recorded ring-downs of the light escaping the cavity. In Fig. 6b, the resulting ring-down times of all 29 recorded ring-down events are shown. The evaluation of all ring-down events results in the following ring-down time and the corresponding cavity finesse:

$$\tau = (742 \pm 21) \text{ ns}, \quad \mathcal{F} = (11,655 \pm 330). \tag{2}$$

This result is more than a factor of four larger than the previous record finesse of a meta-mirror (2784<sup>40</sup>). Thus, this result marks an important step toward the realization of laser

stabilization using low-noise meta-mirrors. The optical losses of the meta-etalon can be calculated from the finesse to be 539 ppm. This corresponds to a minimum reflectivity of 99.95%. A cavity consisting of two etalon mirrors would then theoretically yield a finesse of 6000 (cf. previous record 1500<sup>40</sup>). The finesse of the currently most frequency-stable cavities are even two orders of magnitude higher than those demonstrated here. The finesse of 10<sup>4</sup> presented here is probably limited by scattering losses of the microstructured surface, also leading to limited cavity contrast. These losses are due to the roughness of the structures (compare Methods Fabrication of the Meta Mirror). Further development of this technology has to deal intensively with a reduction of the surface roughness and the associated scattering losses.

**Stability calculation.** To investigate the potential of the mirror presented here, the achievable frequency stability of a cavity equipped with these mirrors will be examined below. The following model system will be used for this purpose: Our model cavity consists of two identical meta-etalon mirrors connected by a crystalline silicon spacer of 21 cm length<sup>6,18</sup> (compare Fig. 1). The beam parameters are also identical to those in previous ultra-stable lasers<sup>6,18</sup>. The model system shall be operated at a temperature of 124 K, so that length fluctuations of the spacer due to temperature variations are reduced to a minimum<sup>6</sup>. The frequency stability of the currently most stable laser cavities is limited by coating Brownian noise<sup>6,18</sup>. In the case of using meta-etalon mirrors, also the thermo-optic noise<sup>30,41</sup>, introduced by local thermal fluctuations coupling to the mirror thickness or refractive index must be considered.

The following noise sources are investigated: Brownian noise of the microstructured surfaces, Brownian noise of the etalon substrates, Brownian noise of the amorphous Bragg layers, thermo-elastic noise of the microstructured surfaces, thermo-elastic noise of the etalon substrates, thermo-elastic noise of amorphous Bragg layers, thermo-refractive noise of microstructured surfaces, thermo-refractive noise of etalon substrates, thermo-refractive noise of amorphous Bragg layers. The Brownian noise of the etalon substrate dominates the total noise of the cavity, because the fused silica has a large mechanical loss at cryogenic temperatures<sup>42</sup>. For large integration times, the thermo-optic noise of the etalon substrate dominates. In the most sensitive range of integration times around 100 ms, the theoretically achievable fundamental noise in terms of frequency stability is  $5 \times 10^{-18}$ , which is one order of magnitude lower than the fundamental noise of most stable laser cavities to date<sup>6,18</sup>. Using crystalline materials as mirror substrates like sapphire, the fundamental noise in terms of frequency stability could be further enhanced to reach  $10^{-18}$  by reduction of Brownian substrate noise (due to lower mechanical losses)<sup>30</sup>.

In our analysis, we assumed that all technical noise sources can be reduced below the fundamental limit calculated here<sup>6,18</sup>. In particular, multistage temperature stabilization, active vibration isolation, and a residual gas pressure of less than  $10^{-9}$  mbar are basic requirements to achieve this stability. In addition, active methods must be used to cancel residual amplitude modulation (RAM)<sup>43</sup>. RAM is particularly problematic at small finesse <100,000<sup>44</sup>. Therefore, in addition to further improving cavity finesse, future studies should analyze the technical sources of noise and methods to suppress them.

## Conclusion

In this work, we reported on the first experimental realization of a high-finesse laser cavity based on a low-noise meta-mirror. We performed a comprehensive preliminary characterization of the meta-etalon, which revealed a broad antiresonance that can be exploited by its high reflectivity. Especially the reflectivity tunability via the angle of polarization is a decisive advantage compared to Bragg mirrors. We have set the world record for finesse of a cavity based on a meta-mirror: The cavity ring-down measurement demonstrated a cavity

finesse of more than 10,000. The fundamental noise analysis of the mirror presented here is very promising and motivates further research on this concept. In particular, the further increase of the finesse and experimental analysis of technical noise sources are in focus. It turns out that the etalon substrate dominates the fundamental noise in terms of frequency stability. Future use of crystalline materials such as sapphire could improve the fundamental noise of the cavity even further to cross the  $10^{-18}$ . These results mark a milestone in the development of next-generation ultra-stable lasers. The use of the technology presented here is of great importance for fundamental research, especially for the detection of gravitational waves, high-precision time measurement and the search for dark matter.

## Methods

**Fabrication of the meta-mirror.** In the first step, hydrogenated amorphous silicon (a-Si:H) without doping is deposited by plasma-enhanced chemical vapor deposition (PECVD) onto a double-side polished fused silica substrate. Next, the film thickness is trimmed to 165 nm by iterative processes of Ion beam etching and ellipsometric thickness measurement. Afterward, 30 nm of chromium is deposited by means of ion beam deposition (Oxford Ionfab 300LC). As a resist mask 100 nm ARP 6200 (Allresist) was used. This was then structured by character projection electron beam lithography<sup>45,46</sup>. Afterward, the chromium layer is etched by reactive ion etching (RIE) and subsequently used as a hard mask for the structuring of the subjacent silicon layer by means of Inductively Coupled Plasma (ICP). Finally, the remaining chromium is removed by wet etching.

**Cavity ring-down measurement.** The finesse of a laser cavity is a measure of the spectral width of its modes. The laser is stabilized to one of these cavity modes. Therefore, the finesse is a measure for the stabilizability of the cavity: the higher the finesse, the better it can be stabilized. Furthermore, for a high finesse, the quantum noise decreases.

There are several ways to measure the finesse of a cavity: Direct measurement of the specular reflectivities, spectral measurement of the linewidth and ring-down measurement. For low finesse below coarse 1000, the first two methods are well-suited because a measurable portion of the power is transmitted. For higher finesse above about 1000, direct measurement should not be used unless you have the ability to use large laser powers. The larger the finesse, the more accurate the cavity ring-down will be<sup>38</sup>. In this method, the photon lifetime in the cavity is measured and from this the finesse is determined<sup>34,39</sup>.

$$\mathcal{F} = \frac{\pi c}{L} \tau. \quad (3)$$

The principle of our measurement setup is as follows: The laser light (Keysight Laser 81606A) entering the cavity is switched off by an acousto-optic modulator (SFO4504-T-M080-0.5C8J-3-F2P) at a threshold voltage, which is measured by a DC photodiode (Thorlabs PDA20CS2) behind the cavity. The transmitted light behind the cavity is also directed to a CCD camera (Xenics Bobcat-320) via a beam splitter so that the resonant mode is filmed simultaneously. This ensures that only the desired mode is excited—in our case the TEM<sub>00</sub> mode. The setup can measure a minimum reflectivity of a 6 cm cavity at 1550 nm of 99.6%.

## Data availability

The data that support the findings of this study are available from the corresponding author upon reasonable request.

## Code availability

The code that supports the findings of this study is available from the corresponding author upon reasonable request.

Received: 14 July 2022; Accepted: 10 January 2023;  
Published online: 20 January 2023

## References

1. Abbott, B. P. et al. Observation of gravitational waves from a binary black hole merger. *Phys. Rev. Lett.* **116**, 061102 (2016).
2. Harry, G. M. Advanced LIGO: the next generation of gravitational wave detectors. *Class. Quantum Gravity* **27**, 084006 (2010).
3. Aasi, J. et al. Enhanced sensitivity of the LIGO gravitational wave detector by using squeezed states of light. *Nat. Photonics* **7**, 613–619 (2013).



4. Andersen, U. L. Squeezing more out of ligo. *Nat. Photonics* **7**, 589–590 (2013).
5. Aasi, J. et al. Advanced LIGO. *Class. Quantum Gravity* **32**, 074001 (2015).
6. Kessler, T. et al. A sub-40-mHz-linewidth laser based on a silicon single-crystal optical cavity. *Nat. Photonics* **6**, 687–692 (2012).
7. Sahni, V. Dark matter and dark energy. in *The Physics of the Early Universe. Lecture Notes in Physics* (ed. Papantonopoulos, E.) Vol. 653, Chapter 5, 141–179 (Springer, 2004).
8. Backes, K. M. et al. A quantum enhanced search for dark matter axions. *Nature* **590**, 238–242 (2021).
9. Wcislo, P. et al. Experimental constraint on dark matter detection with optical atomic clocks. *Nat. Astron.* **1**, 1–6 (2017).
10. Derevianko, A. & Pospelov, M. Hunting for topological dark matter with atomic clocks. *Nat. Phys.* **10**, 933–936 (2014).
11. Ludlow, A. D., Boyd, M. M., Ye, J., Peik, E. & Schmidt, P. O. Optical atomic clocks. *Rev. Modern Phys.* **87**, 637 (2015).
12. Jiang, Y. Y. et al. Making optical atomic clocks more stable with 10-16-level laser stabilization. *Nat. Photonics* **5**, 158–161 (2011).
13. Pizzocaro, M. et al. Intercontinental comparison of optical atomic clocks through very long baseline interferometry. *Nat. Phys.* **17**, 223–227 (2021).
14. Ghelfi, P. et al. A fully photonics-based coherent radar system. *Nature* **507**, 341–345 (2014).
15. Riemensberger, J. et al. Massively parallel coherent laser ranging using a soliton microcomb. *Nature* **581**, 164–170 (2020).
16. Grop, S. et al. ELISA: a cryocooled 10 GHz oscillator with 10-15 frequency stability. *Rev. Sci. Instrum.* **81**, 025102 (2010).
17. Burt, E. A. et al. Demonstration of a trapped-ion atomic clock in space. *Nature* **595**, 43–47 (2021).
18. Matei, D. G. et al. 1.5  $\mu$  m Lasers with sub-10 mHz linewidth. *Phys. Rev. Lett.* **118**, 263202 (2017).
19. Kessler, T., Legero, T. & Sterr, U. Thermal noise in optical cavities revisited. *J. Opt. Soc. Am. B* **29**, 178–184 (2012).
20. Webster, S. A., Oxborrow, M., Pugla, S., Millo, J. & Gill, P. Thermal-noise-limited optical cavity. *Phys. Rev. A* **77**, 033847 (2008).
21. Clerk, A. A., Devoret, M. H., Girvin, S. M., Marquardt, F. & Schoelkopf, R. J. Introduction to quantum noise, measurement, and amplification. *Rev. Mod. Phys.* **82**, 1155–1208 (2010).
22. Cole, G. D., Zhang, W., Martin, M. J., Ye, J. & Aspelmeyer, M. Tenfold reduction of Brownian noise in high-reflectivity optical coatings. *Nat. Photonics* **7**, 644–650 (2013).
23. Harry, G. M. et al. Thermal noise in interferometric gravitational wave detectors due to dielectric optical coatings. *Class. Quantum Grav.* **19**, 897–917 (2002).
24. Yu, J. et al. Novel noise contributions in crystalline mirror coatings. *EFTF/IFCS*, 1–3 (Paris, France, 2022).
25. Mateus, C. F., Huang, M. C., Deng, Y., Neureuther, A. R. & Chang-Hasnain, C. J. Ultrabroadband mirror using low-index cladded subwavelength grating. *IEEE Photonics Technol. Lett.* **16**, 518–520 (2004).
26. Wang, Y., Gao, S., Wang, K., Li, H. & Skafidas, E. Ultra-broadband, compact, and high-reflectivity circular Bragg grating mirror based on 220 nm silicon-on-insulator platform. *Opt. Express* **25**, 6653 (2017).
27. Kroker, S. et al. Brownian thermal noise in functional optical surfaces. *Phys. Rev. D* **96**, 022002 (2017).
28. Dickmann, J., Rojas Hurtado, C., Nawrodt, R. & Kroker, S. Influence of polarization and material on Brownian thermal noise of binary grating reflectors. *Phys. Lett. Sec. A* **382**, 2275–2281 (2018).
29. Kroker, S., Käsebier, T., Steiner, S., Kley, E. B. & Tünnermann, A. High efficiency two-dimensional grating reflectors with angularly tunable polarization efficiency. *Appl. Phys. Lett.* **102**, 161111 (2013).
30. Dickmann, J. & Kroker, S. Highly reflective low-noise etalon-based meta-mirror. *Phys. Rev. D* **98**, 082003 (2018).
31. Plentz, J. et al. Applicability of an economic diode laser emitting at 980 nm for preparation of polycrystalline silicon thin film solar cells on glass. *Physica Status Solidi (A) Sci.* **214**, 1600882 (2017).
32. Moharam, M. G. & Gaylord, T. K. Rigorous coupled-wave analysis of planar-grating diffraction. *J. Opt. Soc. Am.* **71**, 811–818 (1981).
33. Chateau, N. & Hugonin, J.-P. Algorithm for the rigorous coupled-wave analysis of grating diffraction. *J. Opt. Soc. Am. A* **11**, 1321–1331 (1994).
34. Ismail, N., Kores, C. C., Geskus, D. & Pollnau, M. Fabry-Pérot resonator: spectral line shapes, generic and related Airy distributions, linewidths, finesse, and performance at low or frequency-dependent reflectivity. *Opt. Express* **24**, 16366 (2016).
35. Gurkovsky, A. G. et al. Reducing thermal noise in future gravitational wave detectors by employing Khalilii etalons. *Phys. Lett. A* **375**, 4147–4157 (2011).
36. Gong, Y. & Li, B. High-reflectivity measurement with a broadband diode laser based cavity ring-down technique. *Appl. Phys. B Lasers Opt.* **88**, 477–482 (2007).
37. Gong, Y., Li, B. & Han, Y. Optical feedback cavity ring-down technique for accurate measurement of ultra-high reflectivity. *Appl. Phys. B Lasers Opt.* **93**, 355–360 (2008).
38. Truong, G. W. et al. Near-infrared scanning cavity ringdown for optical loss characterization of supermirrors. *Opt. Express* **27**, 19141 (2019).
39. Sridhar, G., Agarwalla, S. K., Singh, S. & Gantayet, L. M. Cavity ring-down technique for measurement of reflectivity of high reflectivity mirrors with high accuracy. *Pramana - J. Phys.* **75**, 1233–1239 (2010).
40. Brückner, F. et al. Realization of a monolithic high-reflectivity cavity mirror from a single silicon crystal. *Phys. Rev. Lett.* **104**, 163903 (2010).
41. Evans, M. et al. Thermo-optic noise in coated mirrors for high-precision optical measurements. *Phys. Rev. D* **78**, 102003 (2008).
42. Nawrodt, R. *Kryogene Gütemessung an optischen Substratmaterialien für zukünftige Gravitationswellendetektoren*. Ph.D. thesis, Friedrich Schiller University Jena (2008).
43. Zhang, W. et al. Reduction of residual amplitude modulation to  $1 \times 10^{-6}$  for frequency modulation and laser stabilization. *Opt. Lett.* **39**, 1980 (2014).
44. Matei, D. G. et al. A second generation of low thermal noise cryogenic silicon resonators. *J. Phys.: Conf. Ser.* **723**, 012031 (2016).
45. Berger, S. D. et al. Projection electron-beam lithography: a new approach. *J. Vac. Sci. Technol. B: Microelectron.* **9**, 2996 (1991).
46. Du, P., Zhao, W., Weng, S. H., Cheng, C. K. & Graham, R. Character design and stamp algorithms for character projection electron-beam lithography. in *Proceedings of the Asia and South Pacific Design Automation Conference, ASP-DAC*, 725–730 (IEEE, 2012).

## Acknowledgements

Funded by the Deutsche Forschungsgemeinschaft (DFG, German Research Foundation) under Germany's Excellence Strategy—EXC-2123 QuantumFrontiers—390837967. J.D. and S.K. also acknowledge partial support by European Association of National Metrology Institutes. This project (20FUN08 NEXTLASERS) has received funding from the EMPIR programme co-financed by the Participating States and from the European Union's Horizon 2020 research and innovation programme. We thank Uwe Sterr (PTB) and Ernst Rasel (LUH) for fruitful discussions.

## Author contributions

J.D.: conceptualization, methodology, investigation, resources, writing, and visualization. S.S.: conceptualization, methodology, and investigation. J.M.: investigation and visualization. M.G.: methodology and investigation. T.S.: investigation, resources, and writing. U.B.: investigation, resources, and writing. J.P.: investigation, resources, and writing. S.K.: conceptualization, resources, writing, and supervision.

## Funding

Open Access funding enabled and organized by Projekt DEAL.

## Competing interests

The authors declare no competing interests.

## Additional information

**Supplementary information** The online version contains supplementary material available at <https://doi.org/10.1038/s42005-023-01131-1>.

**Correspondence** and requests for materials should be addressed to Johannes Dickmann.

**Peer review information** *Communication Physics* thanks the anonymous reviewers for their contribution to the peer review of this work. Peer reviewer reports are available.

**Reprints and permission information** is available at <http://www.nature.com/reprints>

**Publisher's note** Springer Nature remains neutral with regard to jurisdictional claims in published maps and institutional affiliations.



**Open Access** This article is licensed under a Creative Commons Attribution 4.0 International License, which permits use, sharing, adaptation, distribution and reproduction in any medium or format, as long as you give appropriate credit to the original author(s) and the source, provide a link to the Creative Commons license, and indicate if changes were made. The images or other third party material in this article are included in the article's Creative Commons license, unless indicated otherwise in a credit line to the material. If material is not included in the article's Creative Commons license and your intended use is not permitted by statutory regulation or exceeds the permitted use, you will need to obtain permission directly from the copyright holder. To view a copy of this license, visit <http://creativecommons.org/licenses/by/4.0/>.

© The Author(s) 2023